nature geoscience

Article

https://doi.org/10.1038/s41561-023-01300-5

Megafloods in Europe can be anticipated from observations in hydrologically similar catchments

Received: 3 November 2022

Accepted: 18 September 2023

Published online: 06 November 2023

Check for updates

A list of authors and their affiliations appears at the end of the paper

Megafloods that far exceed previously observed records often take citizens and experts by surprise, resulting in extremely severe damage and loss of life. Existing methods based on local and regional information rarely go beyond national borders and cannot predict these floods well because of limited data on megafloods, and because flood generation processes of extremes differ from those of smaller, more frequently observed events. Here we analyse river discharge observations from over 8,000 gauging stations across Europe and show that recent megafloods could have been anticipated from those previously observed in other places in Europe. Almost all observed megafloods (95.5%) fall within the envelope values estimated from previous floods in other similar places on the continent, implying that local surprises are not surprising at the continental scale. This holds also for older events, indicating that megafloods have not changed much in time relative to their spatial variability. The underlying concept of the study is that catchments with similar flood generation processes produce similar outliers. It is thus essential to transcend national boundaries and learn from other places across the continent to avoid surprises and save lives.

Megafloods that are much larger than floods experienced previously in a given catchment or region can take citizens and local flood managers by surprise, resulting in catastrophic damage and loss of life. For example, the discharge of the July 2021 flood at the Rhine tributaries in Germany, and rivers in the Netherlands, Belgium and Luxembourg, was up to four times larger than any event on record in the region[1], causing almost 200 fatalities and damage in excess of US$40 billion. In this and other cases, the lack of previous local experience of events of this magnitude resulted in insufficient flood defence measures, preparedness and real-time response[1,2].

Because of their rare occurrence, megafloods are difficult to predict. The standard method of estimating the magnitude of potential large floods consists of fitting a probability distribution to long series of flood observations, and extrapolating the distribution to small probabilities[3]. However, long series that include several exceptional events are rarely available. Some estimation methods use flood observations from neighbouring catchments[4] to make up for the brevity of streamflow records; however, this rarely increases the chances of capturing megafloods. Even when such events are observed, accurate discharge estimates are difficult to obtain as the flood wave may partially bypass the gauge and cause difficulties with extrapolating the rating curve. Moreover, the processes that generate extreme floods tend to differ from those that generate smaller and more frequent events[5], making extrapolation notoriously inaccurate. One way of capturing changing flood processes with magnitude is through rainfall–runoff models, but they require long series of precipitation and are also subject to uncertainty[6–8]. Large floods in historic or prehistoric times (palaeofloods) can also be used, although the information available is often not commensurate with the requirements of flood management[9–11].

e-mail: bertola@hydro.tuwien.ac.at

https://doi.org/10.1038/s41561-023-01300-5

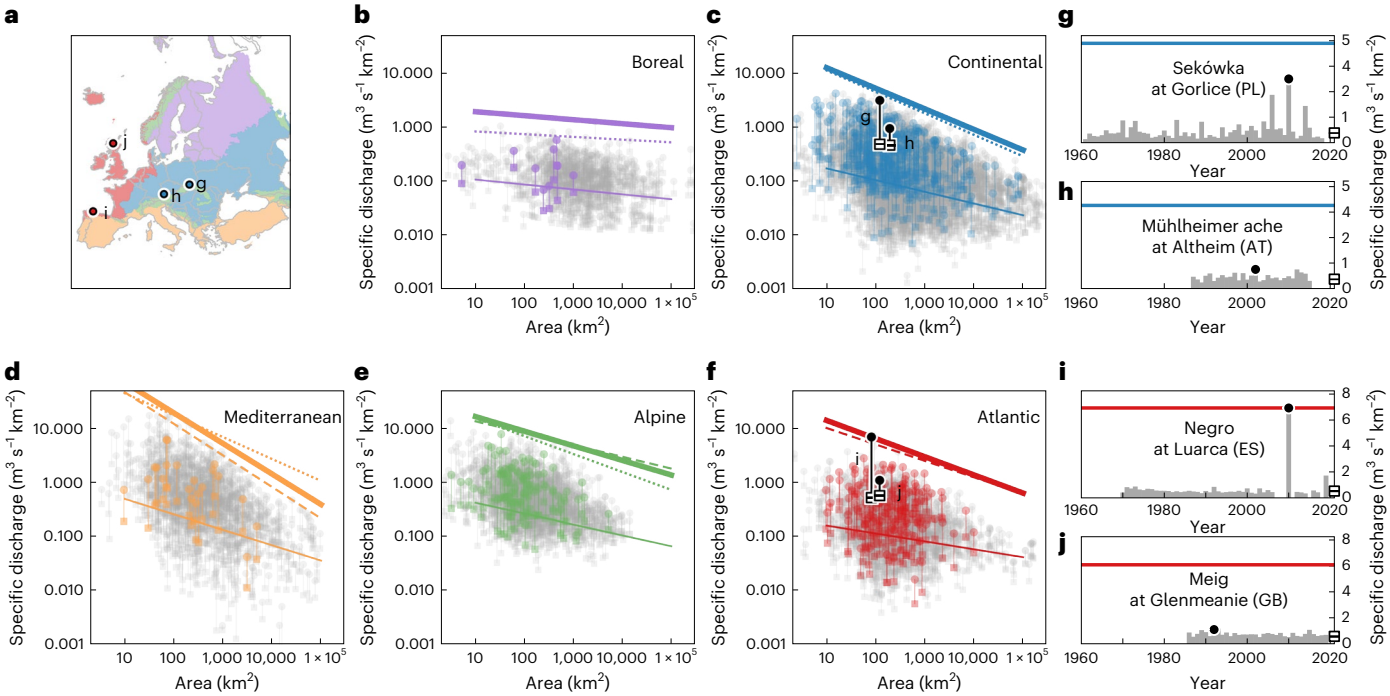

Fig. 1 | Megafloods in Europe. a, Five hydroclimatic regions: Boreal (purple), Continental (blue), Mediterranean (orange), Alpine (green) and Atlantic (red). **b**–**f**, Maximum observed specific flood discharges (points) and mean of annual specific flood discharges (squares) over the entire observation period at each stream gauge as a function of catchment area. Regional envelope curves (thick lines) and median regional annual specific flood discharges (thin lines) for the full record period are shown for each hydroclimatic region: Boreal (**b**), Continental (**c**), Mediterranean (**d**), Alpine (**e**) and Atlantic (**f**). Envelope curves for two 30-year sub-periods are also shown (dashed lines for 1961–1990, dotted lines for 1991–2020). Parameters of the envelope curves are listed in Extended Data Table 2. Coloured symbols indicate the mean and maximum flood discharges in the 498 catchments with recent megafloods, grey points those of the remaining catchments. **g**–**j**, Examples of series of annual flood discharges with (**g**,**i**) and without (**h**,**j**) megafloods; their corresponding mean (squares) and maximum values (points) are highlighted in black in **c** and **f**. The locations of corresponding stream gauges are indicated in **a** by circles. PL, Poland; AT, Austria; ES, Spain; GB, United Kingdom.

An alternative for enhancing the accuracy of megaflood estimates is the transfer of flood information from hydrologically similar catchments where large events may have occurred[4]. In Europe the occurrence of megafloods is well documented at the national scale. The August 2002 flood in Germany, Austria and Bohemia was the largest in the last half century based on economic losses; and the November 1994 Piedmont flood was the second costliest event in Europe between 1970 and 2020[12]. Both events were caused by rainfall greater than one-third of the annual total, delivered in only 72 hours[13,14]. However, flood information transfer rarely goes beyond national borders, and no previous study has examined megafloods in a systematic way across an entire continent, with the objective of learning from other places about the potential of future flood surprises. Some examples comparing the world's maximum measured floods also exist[15], but they do not compare hydrologically similar catchments, which makes flood estimation less useful for practical proposes.

Anticipating megafloods

Here we analyse the most comprehensive dataset of annual maximum discharges in Europe available to date and show that recent megafloods could have been anticipated from observations in other parts of Europe, which would not be possible using only national data. We also show that the predictability of megafloods does not change in time when sub-periods are analysed. We base our analysis on annual maximum river discharge observations from 8,023 gauging stations for the period 1810–2021. The average length of the series is 51.4 years and the catchment areas range between 1 and 800,000 km^2. Catchments across Europe are grouped into five hydroclimatic regions (Fig. 1) as a first step in identifying hydrologically similar catchments[16]. For each region, we estimate a regional envelope curve of flood discharges that represents the relationship between flood discharge and catchment area that is not exceeded by any observed flood in the region (Methods and Extended Data Table 2). To examine possible changes in time, we also compare envelope curves obtained using observations from two 30-year sub-periods, that is, 1961–1990 and 1991–2020.

We focus on 498 catchments ('target' catchments) where 510 recent (that is, after 1999) megafloods that are surprising based on local data are identified (Methods). To evaluate the possibility of anticipating megafloods in target catchments using information from other places in Europe, we perform a hindcast experiment of predicting their peak discharge with regional envelope curves, using flood observations from similar catchments up to the year before their occurrence. For each target catchment, a group of similar catchments ('donor' catchments) is identified in the corresponding hydroclimatic region based on the similarity of catchment area, and the mean and coefficient of variation of the truncated flood series (up to the year before the megaflood). From this group of donor catchments we construct an envelope curve, which we compare with the megaflood that occurred later in the target catchments. We repeat this analysis for all 510 detected megafloods in the target catchments.

European envelope curves of flood discharges

Our data show that recent megafloods have occurred in all regions of Europe, although they are more frequent in the Atlantic and Continental regions (Fig. 1 and Extended Data Table 3), where respectively 8.7% and 7.2% of the catchments exhibit recent megafloods. In the Boreal region, the respective value is only 1.3%. The smaller value is related to the smaller interannual variability of floods in the Boreal region[17].

https://doi.org/10.1038/s41561-023-01300-5

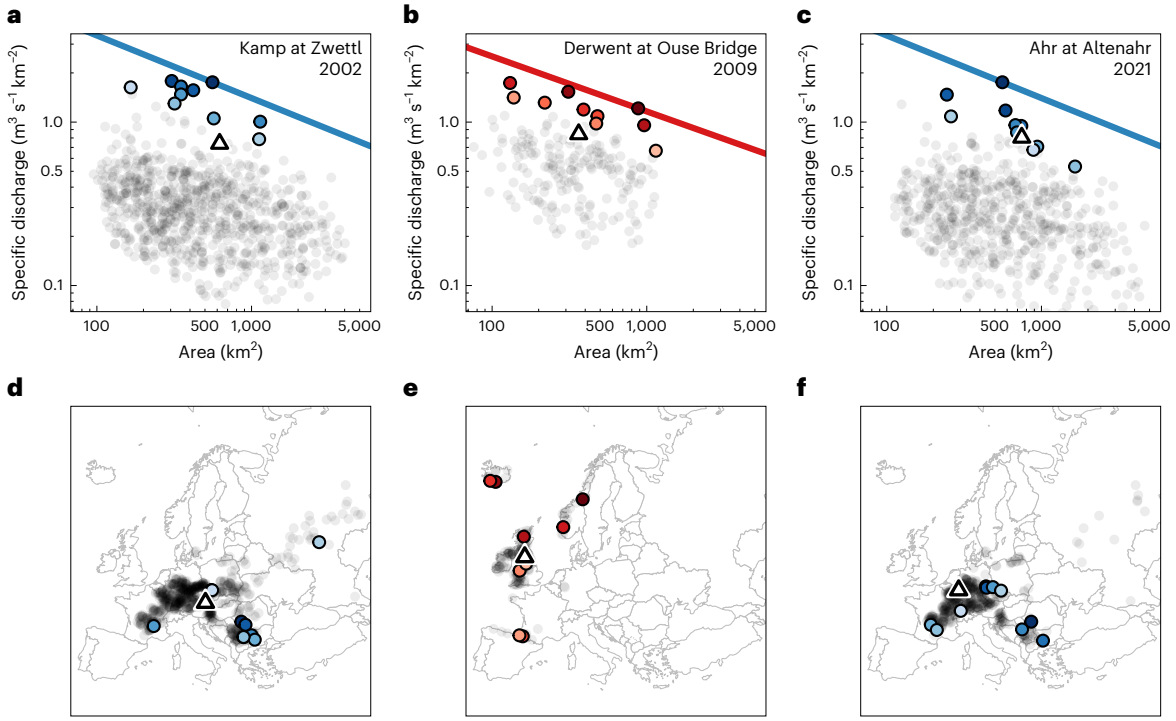

Fig. 2 | Envelope curves for three catchments with recent megafloods in Europe. a–f, Kamp (622 km² catchment area) with 2002 flood (**a**,**d**), Cumbrian Derwent (363 km²) with 2009 flood (**b**,**e**) and Ahr (746 km²) with 2021 flood (**c**,**f**), indicated with triangles. Maximum specific discharges observed before the year of occurrence of the megaflood for are shown for 824 (**a**), 196 (**b**) and 590 (**c**) similar donor catchments (points) selected within the corresponding hydroclimatic region. Coloured points indicate the ten largest events (in terms of distance to the envelope curve), with shades being darker for events that are closer to the envelope. The line shows the resulting envelope curve with the slope estimated from the hydroclimatic regions (Fig. 1b–f). Locations of the target (triangle) and donor (points) catchments are shown in **d**–**f**. Note that the envelope curves of Fig. 1 refer to the entire hydroclimatic region, while here they refer to the donor group within a region.

In the Atlantic region, the megafloods (coloured points in Fig. 1b–f) are on average 3.4 times larger than the local mean annual maximum discharges (squares), while in the Continental and Mediterranean regions they are 5.3 and 5.2 times larger, respectively (Extended Data Table 3). The larger ratio in the Mediterranean is probably related to the more nonlinear rainfall–runoff process and more variable precipitation in arid than in humid climates[5,18]. However this analysis is not able to conclude whether megafloods are becoming more frequent or not.

The envelope curves defined by the largest floods also differ between hydroclimatic regions in terms of their intercept and slope (thick continuous lines in Fig. 1b–f; Extended Data Table 2). For a catchment size of 1,000 km², the envelope-specific discharge in the Mediterranean region is 5.26 $m^3 s^{-1} km^{-2}$, while in the Boreal region it is 1.37 $m^3 s^{-1} km^{-2}$. This is because the flood-inducing rainstorms in the Mediterranean are associated with much larger intensities than the flood-inducing snowmelt typical of Northern Europe. The slopes of the envelope curves are steepest in the Mediterranean area (−0.57) and flattest (−0.07) in the Boreal region (Fig. 1). This is because the Mediterranean rainstorms tend to be more localized than the snowmelt in the north of Europe. The envelope curves for the most recent sub-period (thin dotted lines) tend to be slightly lower than those for the first sub-period (thin dashed lines), except for the Mediterranean and the Atlantic region. The median regression curves (thin continuous lines) are slightly flatter than the respective envelopes, as larger catchments tend to have more regular flood regimes than small ones. Figure 1g–j illustrates examples of flood series in pairs of catchments with and without megafloods.

To illustrate the potential of anticipating megafloods from other places in Europe, Fig. 2 shows three examples. The 2002 flood in the Kamp catchment in Austria (Fig. 2a) peaked at 459 $m^3 s^{-1}$, which is equivalent to a specific discharge of 0.74 $m^3 s^{-1} km^{-2}$ (black triangle) given the catchment area of 622 km². The envelope curve (blue line), defined by the hydrologically similar catchments within the hydroclimatic region, gives a specific discharge of 1.68 $m^3 s^{-1} km^{-2}$. This means that, in light of European floods, the Kamp was not at all surprising, while for the locals it was[19]. The regional envelope discharge illustrated in Fig. 2 is defined based on previously observed floods in various European countries, including Bulgaria and Poland (blue circles in Fig. 2d).

The 2009 flood in the Cumbrian Derwent catchment in the UK (Fig. 2b) peaked at 0.84 $m^3 s^{-1} km^{-2}$ and was 58% larger than the second largest event on record, which occurred in 2005. The corresponding envelope-specific discharge is 1.64 $m^3 s^{-1} km^{-2}$. Much larger extremes were observed in similar catchments in Norway (Fig. 2e). The 2009 megaflood in the Derwent was itself exceeded in 2015; however, this later event still lies below the envelope curve and was not as surprising as the 2009 event (11% larger)[2].

The 2021 flood in the Ahr catchment in Germany (Fig. 2c) peaked at 0.80 $m^3 s^{-1} km^{-2}$, similar to the Kamp flood, with an envelope estimate of 1.57 $m^3 s^{-1} km^{-2}$. For the Ahr catchment, the similar catchments making up the donor group are, in descending order of flood magnitude: the Timis in Romania, the Freiberger Mulde in Germany, the Maritsa in Bulgaria, the Ljig in Serbia, the Lausitzer Neisse in Germany, the Corrèze and Le Lot in France, the Nysa Kłodzka in Poland and the Birs in Switzerland (Fig. 3). Although each of these catchments has a specific hydrological behaviour, overall they can be considered hydrologically similar to the Ahr in terms of average climate and flood statistical properties. All of these ten catchments experienced record-breaking floods that were surprising based on previously observed events at that location, and these occurred in the period before 2021 (Fig. 3).

The analysis of Fig. 2 is repeated for all 510 recent megafloods in the target catchments in Europe (Fig. 4). In 95.5% of the target catchments,

https://doi.org/10.1038/s41561-023-01300-5

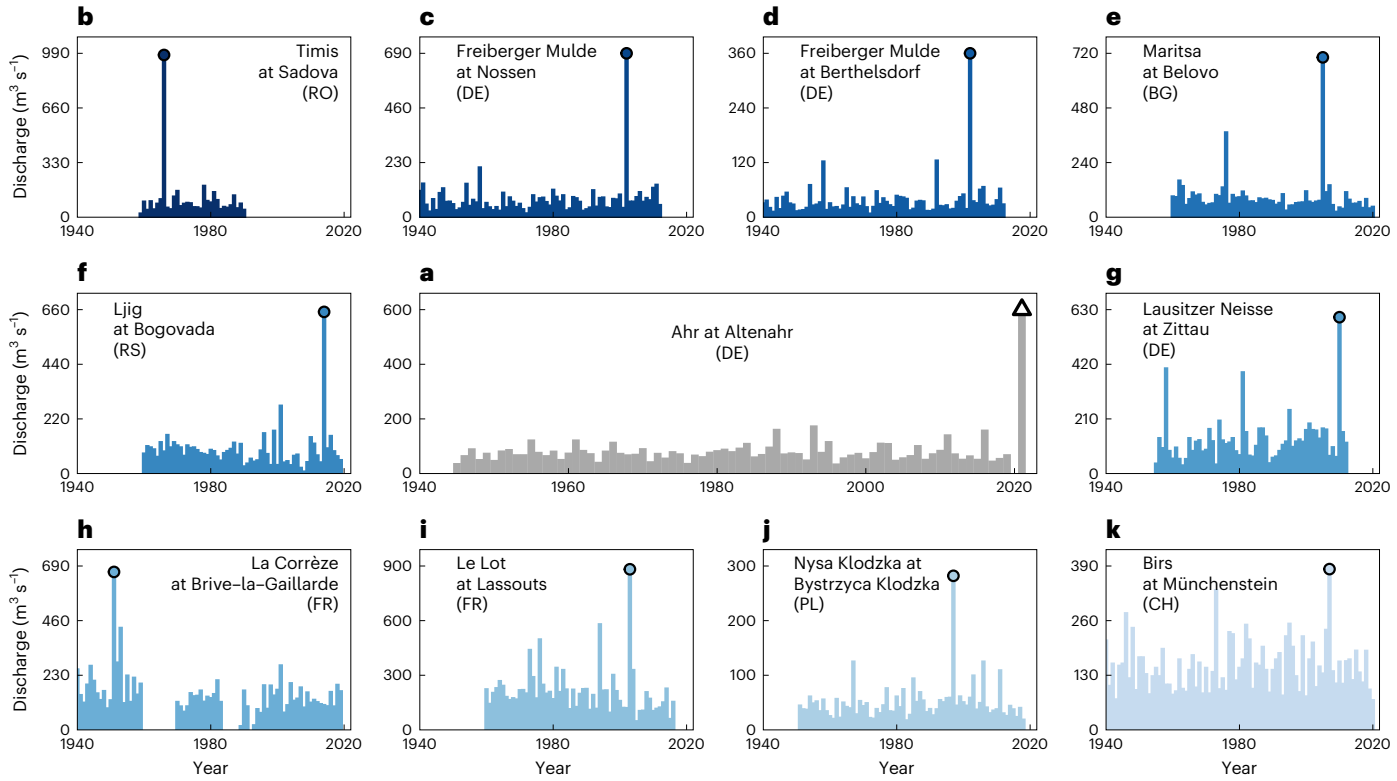

Fig. 3 | Annual flood series for the Ahr and ten donor catchments with extreme floods. a, Ahr at Altenahr, Germany, with the 2021 megaflood (the target event) indicated as a triangle. **b**–**k**, Series for the ten donor catchments indicated as coloured dots in Fig. 2c,f. RO, Romania; DE, Germany; BG, Bulgaria; RS, Serbia; FR, France; PL, Poland; CH, Switzerland.

the discharge of the envelope is larger than that of the observed megaflood, suggesting that, from a European perspective, almost none of the events can be considered a regional surprise. In 9.6% of the cases, the observed megafloods are within 75% and 150% of the envelope (red points in Fig. 4a), that is, the order of magnitude is similar. The target catchments are distributed all over Europe, with a higher concentration in the west (Fig. 4b), reflecting positive trends in flood magnitudes in Western Europe[20,21] and, to some degree, the higher station density.

The prediction is also conducted for 151 and 188 catchments with 151 and 190 recent (that is, in the past ten years of each sub-period) megafloods in the first and second sub-period, respectively. The distribution of the ratio between observed and predicted discharge (inset of Fig. 4a) indicates that there are no substantial changes in the predictability of megafloods in time. The discharge of the envelope is larger than that of the observed megaflood in 92% and 93.7% of the respective target catchments.

To evaluate the suitability of the donor selection, we compare the timing within the year of the target megafloods with that of the ten largest floods in the donor catchments (Fig. 4c). Flood timing is a proxy of flood generation processes[22]. Figure 4c shows that the timing of the target megafloods (black lines) generally agrees with that of the donors (brown lines), both in terms of the average timing (angle from the centre of the circle) and the consistency of timing between events (distance to the centre). The agreement points towards the plausibility of the donor selection and prediction. A tendency for the observed timings to be more bimodal than the predictions is probably related to the smaller number of events.

Implications of expanding the perspective

Whereas previous studies have assessed the potential for megafloods mainly based on local or regional data, this study expands the observation area to the continental scale. We use megafloods that have occurred in hydrologically similar catchments elsewhere on the continent as a surrogate for the megafloods that could happen in the catchment of interest in the future.

The degree to which this transfer of information is possible depends on the suitable choice of donor catchments based on the notion of hydrological similarity[23]. The underlying concept is that catchments with similar flood generation processes, including rainfall, infiltration and flow paths, produce similar outliers, as these processes determine the transition from smaller to larger events[5,24,25]. Here we use catchment area and the mean and coefficient of variation of the truncated flood series within the same hydroclimatic region as a proxy of similarity in flood generation processes. While other similarity measures exist[16], our donor catchment selection is deemed plausible because of the similarity of the timing within the year of the events, given that timing is a fingerprint of the interplay between climatic and catchment processes[22]. Additional spot testing of catchment pairs (such as the Ahr catchment in Germany paired with the Timis catchment in Romania) based on prior knowledge from the literature[1,25] confirms the similarity. To assess robustness of the method, we conduct a sensitivity analysis on the parameters of the similarity criteria and the choice of hydroclimatic regions (Extended Data Figs. 1–7). The results show that changing parameters and/or regions may modify individual donor catchments, but the envelope curve that arises from the set of donor catchments is affected much less (Methods).

The cross-validation experiment conducted here, starting from observed megafloods, withholding them and only using data from floods that have occurred previously, mimics the case of anticipating megafloods that have not yet occurred. We show that it is indeed feasible to estimate the order of magnitude of possible future megafloods. Almost all observed megafloods (95.5%) are smaller than the envelope values estimated, that is, the local surprises are not surprising at the continental scale. Similar results are found for different sub-periods,

https://doi.org/10.1038/s41561-023-01300-5

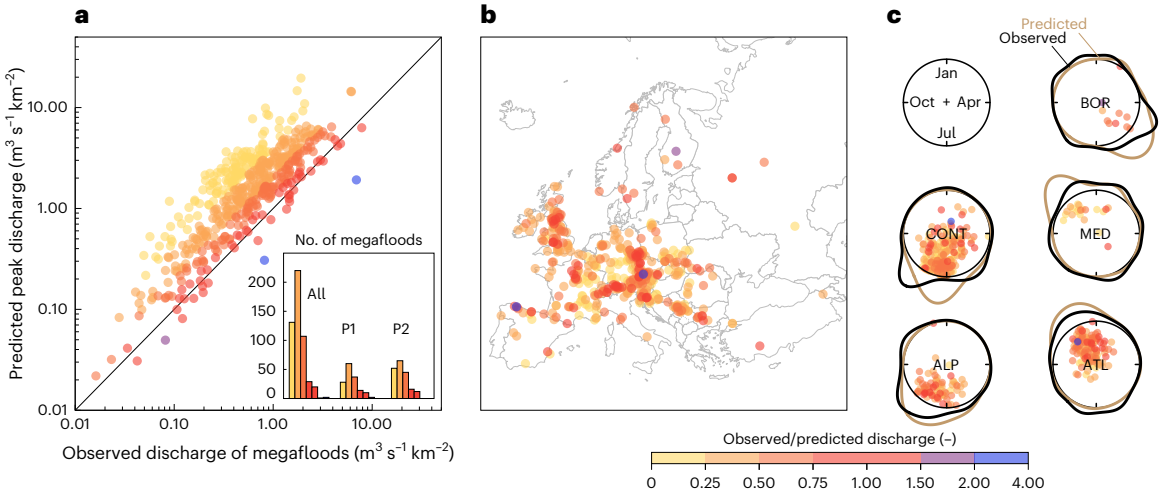

Fig. 4 | Predicted versus observed megafloods. a, Predicted specific envelope discharge for 498 target catchments versus observed specific discharge of the megafloods in the same catchments. Predicted envelope discharges are estimated using discharge observations from a pool of donor catchments up to the year before the target megaflood. The number of target megafloods is shown in the inset for the entire period ('All') and the two sub-periods 1961–1990 ('P1') and 1991–2020 ('P2'). Colours indicate the ratio of observed and predicted discharge. **b**, Location of target catchments. Megafloods occur all over Europe and are less surprising than commonly assumed. **c**, Circular distribution of the timing of the megafloods observed in the target catchments (black lines), and mean timing of the ten largest floods in the donor catchments (coloured points) and their distribution (brown lines). The distance of the points to the centre is inversely proportional to the standard deviation of the flood timing. BOR, Boreal; CONT, Continental; MED, Mediterranean; ALP, Alpine; ATL, Atlantic.

indicating that megafloods have not changed much in time relative to their spatial variability within Europe. These findings are in line with recent studies in the USA showing little evidence for temporal trends of large floods[26].

The proposed envelope curve approach complements alternative methods, such as regional statistical approaches that spatially interpolate observed discharges[4] or process-based rainfall–runoff modelling[27]. These methods provide best estimates of expected floods, while the envelope method reflects a possible worst case—which itself is an important aspect of flood risk planning.

The focus on a possible worst case implies that the envelope values are generally too large to serve as design values for most types of flood defence infrastructure from a cost–benefit perspective. Rather, they describe a 'possibility space'[28] that is prudent to consider in civil protection scenarios, which are required to organize local preparedness, and for testing the safety of very large dams. They can be used to derive extreme flood hazard scenarios, either failure scenarios (what can go wrong?) or future development scenarios (what could the future look like?) that could strengthen existing methods such as the probable maximum flood concept[29]. There is an increasing need for considering the extremes of the extremes, as there is a tendency in society for smaller acceptable risks[29], so flood risk management should account for the potential of surprises and their devastating consequences. This requires a shift in thinking[29] and the application of envelope curves, storylines[2,30] and compound event analyses[31]. Making individuals and societies more robust against surprises therefore goes beyond the design of spillways and flood management plans.

In summary, to anticipate megafloods we must learn from other places in order to reduce the surprise factor of their occurrence, increase flood risk awareness and enhance preparedness of flood risk management. To this end, it is essential to move beyond national flood risk assessment and share information on megafloods across countries and continents.

Online content

Any methods, additional references, Nature Portfolio reporting summaries, source data, extended data, supplementary information, acknowledgements, peer review information; details of author contributions and competing interests; and statements of data and code availability are available at https://doi.org/10.1038/s41561-023-01300-5.

References

1. Apel, H., Vorogushyn, S. & Merz, B. Brief communication: Impact forecasting could substantially improve the emergency management of deadly floods: case study July 2021 floods in Germany. *Nat. Hazards Earth Syst. Sci.* **22**, 3005–3014 (2022).
2. Kreibich, H. et al. The challenge of unprecedented floods and droughts in risk management. *Nature* **608**, 80–86 (2022).
3. De Niel, J., Demarée, G. & Willems, P. Weather typing based flood frequency analysis validated for exceptional historical events of past 500 years along the Meuse River. *Water Resour. Res.* **53**, 8459–8474 (2017).
4. Robson, A. J. & Reed, D. W. *Flood Estimation Handbook*, Vol. 3 (Centre for Ecology & Hydrology, 1999).
5. Rogger, M. et al. Step changes in the flood frequency curve: process controls. *Water Resour. Res.* **48**, W05544. (2012).
6. Bergstrand, M., Asp, S. & Lindström, G. Nationwide hydrological statistics for Sweden with high resolution using the hydrological model S-HYPE. *Hydrol. Res.* **45.3**, 349–356 (2014).
7. Devitt, L., Neal, J., Wagener, T. & Coxon, G. Uncertainty in the extreme flood magnitude estimates of large-scale flood hazard models. *Environ. Res. Lett.* **16**, 064013 (2021).
8. Bouaziz, L. et al. Behind the scenes of streamflow model performance. *Hydrol. Earth Syst. Sci.* **25**, 1069–1095 (2021).
9. Kjeldsen, T. R. et al. Documentary evidence of past floods in Europe and their utility in flood frequency estimation. *J. Hydrol.* **517**, 963–973 (2014).
10. Blöschl, G. et al. Current European flood-rich period exceptional compared with past 500 years. *Nature* **583**, 560–566 (2020).
11. Ryberg, K. R., Kolars, K. A., Kiang, J. E. & Carr, M. L. *Flood-Frequency Estimation for Very Low Annual Exceedance Probabilities Using Historical, Paleoflood, and Regional Information with Consideration of Nonstationarity* (USGS, 2020).
12. *WMO Atlas of Mortality and Economic Losses from Weather, Climate and Water Extremes (1970–2019)* WMO-No. 1267 (WMO, 2021).

13. Blöschl, G., Nester, T., Komma, J., Parajka, J. & Perdigão, R. A. P. The June 2013 flood in the Upper Danube Basin, and comparisons with the 2002, 1954 and 1899 floods. *Hydrol. Earth Syst. Sci.* **17**, 5197–5212 (2013).
14. Lionetti, M. The Italian floods of 4–6 November 1994. *Weather* **51**, 18–27 (1996).
15. Herschy, R. W. The world's maximum observed floods. *Flow. Meas. Instrum.* **13**, 231–235 (2002).
16. Kuentz, A., Arheimer, B., Hundecha, Y. & Wagener, T. Understanding hydrologic variability across Europe through catchment classification. *Hydrol. Earth Syst. Sci.* **21**, 2863–2879 (2017).
17. Lun, D. et al. Characteristics and process controls of statistical flood moments in Europe – a data-based analysis. *Hydrol. Earth Syst. Sci.* **25**, 5535–5560 (2021).
18. Blöschl, G. Flood generation: process patterns from the raindrop to the ocean. *Hydrol. Earth Syst. Sci.* **26**, 2469–2480 (2022).
19. Blöschl, G. Flood warning - on the value of local information. *Int. J. River Basin Manag.* **6**, 41–50 (2008).
20. Blöschl, G. et al. Changing climate both increases and decreases European river floods. *Nature* **573**, 108–111 (2019).
21. Bertola, M., Viglione, A., Lun, D., Hall, J. & Blöschl, G. Flood trends in Europe: are changes in small and big floods different? *Hydrol. Earth Syst. Sci.* **24**, 1805–1822 (2020).
22. Blöschl, G. et al. Changing climate shifts timing of European floods. *Science* **357**, 588–590 (2017).
23. Blöschl, G., Sivapalan, M., Wagener, T., Viglione, A. & Savenije, H. H. (eds) *Runoff Prediction in Ungauged Basins: Synthesis across Processes, Places and Scales* (Cambridge Univ. Press, 2013).
24. Kemter, M., Merz, B., Marwan, N., Vorogushyn, S. & Blöschl, G. Joint trends in flood magnitudes and spatial extents across Europe. *Geophys. Res. Lett.* **47**, e2020GL087464 (2020).
25. Popescu, I., Jonoski, A., Van Andel, S. J., Onyari, E. & Moya Quiroga, V. G. Integrated modelling for flood risk mitigation in Romania: case study of the Timis–Bega River Basin. *Int. J. River Basin Manag.* **8**, 269–280 (2010).
26. Collins, M. J., Hodgkins, G. A., Archfield, S. A. & Hirsch, R. M. The occurrence of large floods in the United States in the modern hydroclimate regime: seasonality, trends, and large-scale climate associations. *Water Resour. Res.* **58**, e2021WR030480 (2022).
27. Donnelly, C., Andersson, J. C. M. & Arheimer, B. Using flow signatures and catchment similarities to evaluate a multi-basin model (E-HYPE) across Europe. *Hydr. Sci. J.* **61**, 255–273 (2016).
28. Sivapalan, M. & Blöschl, G. Time scale interactions and the coevolution of humans and water. *Water Resour. Res.* **51**, 6988–7022 (2015).
29. Merz, B., Vorogushyn, S., Lall, U., Viglione, A. & Blöschl, G. Charting unknown waters—On the role of surprise in flood risk assessment and management. *Water Resour. Res.* **51**, 6399–6416 (2015).
30. Shepherd, T. G. Storyline approach to the construction of regional climate change information. *Proc. R. Soc. A* **475**, 20190013 (2019).
31. Thieken, A. H., Samprogna Mohor, G., Kreibich, H. & Müller, M. Compound inland flood events: different pathways, different impacts and different coping options. *Nat. Hazards Earth Syst. Sci.* **22**, 165–185 (2022).

Miriam Bertola[1] ✉, Günter Blöschl[1], Milon Bohac[2], Marco Borga[3], Attilio Castellarin[4], Giovanni B. Chirico[5], Pierluigi Claps[6], Eleonora Dallan[3], Irina Danilovich[7], Daniele Ganora[6], Liudmyla Gorbachova[8], Ondrej Ledvinka[2,9], Maria Mavrova-Guirguinova[10], Alberto Montanari[4], Valeriya Ovcharuk[11], Alberto Viglione[6], Elena Volpi[12], Berit Arheimer[13], Giuseppe Tito Aronica[14], Ognjen Bonacci[15], Ivan Čanjevac[16], Andras Csik[17], Natalia Frolova[18], Boglarka Gnandt[17], Zoltan Gribovszki[19], Ali Gül[20], Knut Günther[21], Björn Guse[21,22], Jamie Hannaford[23,24], Shaun Harrigan[25], Maria Kireeva[18], Silvia Kohnová[26], Jürgen Komma[1], Jurate Kriauciuniene[27], Brian Kronvang[28], Deborah Lawrence[29], Stefan Lüdtke[21], Luis Mediero[30], Bruno Merz[21,31], Peter Molnar[32], Conor Murphy[24], Dijana Oskoruš[33,34], Marzena Osuch[35], Juraj Parajka[1], Laurent Pfister[36], Ivan Radevski[37], Eric Sauquet[38], Kai Schröter[39], Mojca Šraj[40], Jan Szolgay[26], Stephen Turner[23], Peter Valent[1], Noora Veijalainen[41], Philip J. Ward[42,43], Patrick Willems[44] & Nenad Zivkovic[45]

[1]Institute of Hydraulic Engineering and Water Resources Management, Technische Universität Wien, Vienna, Austria. [2]Czech Hydrometeorological Institute, Prague, Czechia. [3]Department of Land, Environment, Agriculture and Forestry, University of Padova, Padua, Italy. [4]Department of Civil, Chemical, Environmental and Materials Engineering (DICAM), Università di Bologna, Bologna, Italy. [5]Department of Agricultural Sciences, University of Naples Federico II, Naples, Italy. [6]Department of Environment, Land and Infrastructure Engineering (DIATI), Politecnico di Torino, Turin, Italy. [7]Climate Research Laboratory, Institute for Nature Management, The National Academy of Science of Belarus, Minsk, Belarus. [8]Department of Hydrological Research, Ukrainian Hydrometeorological Institute, Kyiv, Ukraine. [9]Department of Physical Geography and Geoecology, Faculty of Science, Charles University, Prague, Czechia. [10]University of Architecture, Civil Engineering and Geodesy, Sofia, Bulgaria. [11]Hydrometeorological Institute, Odessa State Environmental University, Odessa, Ukraine. [12]Department of Engineering, University Roma Tre, Rome, Italy. [13]Swedish Meteorological and Hydrological Institute, Norrköping, Sweden. [14]Department of Engineering, University of Messina, Messina, Italy. [15]Faculty of Civil Engineering, Architecture and Geodesy, Split University, Split, Croatia. [16]Department of Geography, Faculty of Science, University of Zagreb, Zagreb, Croatia. [17]General Directorate of Water Management, Budapest, Hungary. [18]Department of Land Hydrology, Lomonosov Moscow State University, Moscow, Russia. [19]Faculty of Forestry, Institute of Geomatics and Civil Engineering, University of Sopron, Sopron, Hungary. [20]Department of Civil Engineering, Faculty of Engineering, Dokuz Eylul University, Izmir, Turkey. [21]Section Hydrology, GFZ German Research Centre for Geosciences, Helmholtz Centre Potsdam, Potsdam, Germany. [22]Department of Hydrology and Water Resources Management, Institute for Natural Resource Conservation, Kiel University, Kiel, Germany. [23]Centre for Ecology and Hydrology, Wallingford, UK. [24]Irish Climate Analysis and Research Units (ICARUS), Department of Geography, Maynooth University, Maynooth, Ireland. [25]Forecast Department, European Centre for Medium-Range Weather Forecasts (ECMWF), Reading, UK. [26]Department of Land and

Water Resources Management, Faculty of Civil Engineering, Slovak University of Technology in Bratislava, Bratislava, Slovakia. [27]Lithuanian Energy Institute, Kaunas, Lithuania. [28]Department of Ecoscience, Danish Centre for Environment and Energy, Aarhus University, Aarhus, Denmark. [29]Norwegian Water Resources and Energy Directorate, Oslo, Norway. [30]Department of Civil Engineering: Hydraulic, Energy and Environment, Universidad Politécnica de Madrid, Madrid, Spain. [31]Institute of Environmental Sciences and Geography, University Potsdam, Potsdam, Germany. [32]Institute of Environmental Engineering, ETH Zurich, Zurich, Switzerland. [33]Department of Hydrotechnics, Faculty of Geotechnical Engineering, University of Zagreb, Varaždin, Croatia. [34]Croatian Meteorological and Hydrological Service, Zagreb, Croatia. [35]Department of Hydrology and Hydrodynamics, Institute of Geophysics Polish Academy of Sciences, Warsaw, Poland. [36]Luxembourg Institute of Science and Technology (LIST), Esch-sur-Alzette, Luxembourg. [37]Institute of Geography, Faculty of Natural Sciences and Mathematics, Ss. Cyril and Methodius University, Skopje, North Macedonia. [38]Irstea, UR RiverLy, Lyon-Villeurbanne, France. [39]Leichtweiss Institute for Hydraulic Engineering and Water Resources, Technische Universität Braunschweig, Braunschweig, Germany. [40]Faculty of Civil and Geodetic Engineering, University of Ljubljana, Ljubljana, Slovenia. [41]Finnish Environment Institute, Helsinki, Finland. [42]Institute for Environmental Studies (IVM), Vrije Universiteit Amsterdam, Amsterdam, The Netherlands. [43]Deltares, Delft, The Netherlands. [44]Department of Civil Engineering, KU Leuven, Leuven, Belgium. [45]Faculty of Geography, University of Belgrade, Belgrade, Serbia. ✉e-mail: bertola@hydro.tuwien.ac.at

Methods

Datasets

The hydrological data used in this study were obtained from a pan-European Flood Database[32] with subsequent updates. The current version contains data from 8,023 hydrometric gauging stations from 68 European data sources for the period 1810–2021 (Extended Data Table 1). The dataset consists of the highest discharge (daily mean or instantaneous discharge) in each calendar year for each station. The stations are located within the domain bounded by 22.25° W–63.25° E and 34.25° N–71.25° N (Extended Data Fig. 1), and catchment areas range between 1 km^2 and 800,000 km^2. The dataset was screened for data errors. The screening involved visual examination of the flood records, analysis of flood seasonality and examination of the guage location and catchment area in Google Maps. All available stations, including those affected by reservoir construction, were considered for the analysis because reservoir effects were deemed to have little effect on envelope curves for large hydroclimatic regions. Similarly, all available years with data were considered notwithstanding differences in the record lengths, because the focus was on the maxima observations of each series. The minimum series length is 10 years and the average length is 51.4 years.

The gauging stations were grouped into five regions (Fig. 1a and Extended Data Fig. 1) that reflect similar hydroclimatic conditions by generalizing the European Biogeographical Regions[33] with a view on flood processes. The Steppic and Pannonian regions were merged with the Continental region, the Arctic region with the Boreal region, and the Anatolian and Black Sea regions with the Mediterranean region. Additionally, part of northern Italy was considered as part of the Mediterranean region and Iceland as part of the Atlantic region. For comparison, an alternative subdivision of Europe into five regions[17] was considered in a sensitivity analysis (Extended Data Fig. 4a). In order to examine possible changes, the observation period was subdivided into two 30-year sub-periods, P1 (1961–1990) and P2 (1991–2020).

Regional envelope curves

We quantified the largest flood events in each region by scaling the peak discharges by catchment area via envelope curves that represent the upper limit of the dataset (Fig. 1):

$$\log(q) = a + b\log(A) \tag{1}$$

where q (m^3 s^{-1} km^{-2}) is the specific discharge, that is, the discharge per unit catchment area A. The parameter b was estimated by quantile regression with quantile $z = 0.999$ using the rq function of the R quantreg package[34,35]. The quantile regression enables a more robust estimate than the tangents on the maxima, because it uses the complete dataset rather than the maxima only. The intercept a was determined such that it satisfies the envelope condition, that is, the envelope curve is the upper bound of all observed flood discharges in a region (Extended Data Table 2). For comparison, a quantile regression with $z = 0.5$ is also shown in Fig. 1 (thin line).

Megafloods

For the selection of recent megafloods (Fig. 4) the following criteria were adopted:

(1) The discharge value, q_{mf}, is a high outlier in the corresponding series of annual maximum flood discharges, according to the definition[36]:

$$q_{mf} > Q_3 + k(Q_3 - Q_1) \tag{2}$$

where Q_1 and Q_3 are the first and third quartiles, respectively (that is, respectively 25% and 75% of the observations lies below this values), and k is a nonnegative constant. Here we assumed $k = 3$.

(2) The discharge value is record-breaking and locally surprising, that is, its return period T_{mf} is at least 3 times larger than the return period of the second largest event up to that year T_{sl}. The return period was obtained by fitting a generalized extreme value distribution to each flood series up to the year of the megaflood using the L-moments (R extRemes package).

(3) It occurred after the year 1999 (when the full observation period is analysed) and the corresponding series has at least 20 years of data previous to the event.

The selection resulted in a set of 510 megafloods from 498 target catchments, whose observed specific discharge and location of corresponding gauges are shown in Fig. 4a,b. When detecting megafloods in the two 30-year sub-periods, only observations within each sub-period are considered and the criterion (3) is modified such that events in the last 10 years of the respective sub-period are selected (that is, after 1979 for P1 and after 2009 for P2).

We tested the robustness of the results to the criterion (1) for the selection of high outliers, using the definition for skewed data[37]:

$$\begin{cases} q_{mf} > Q_3 + 1.5e^{3MC}\mathrm{IQR} \text{ if } MC > 0 \\ q_{mf} > Q_3 + 1.5e^{4MC}\mathrm{IQR} \text{ if } MC < 0 \end{cases} \tag{3}$$

where IQR is the interquartile range and MC is the medcouple[38], a robust measure of skewness, defined as:

$$\mathrm{MC}(X_n) = \underset{x_i \le m_n \le x_j}{\mathrm{med}} h(x_i, x_j) \tag{4}$$

where m_n is the sample median of n independent observations $X_n = \{x_1, x_2, \ldots, x_n\}$ such that $x_1 \le x_2 \le \ldots \le x_n$, and

$$h(x_i, x_j) = \frac{(x_j - m_n) - (m_n - x_i)}{x_j - x_i} \tag{5}$$

for all couples of indices i and j such that $x_i \le m_n \le x_j$. The alternative selection resulted in a set of 677 megafloods (Supplementary Fig. 1), whose observed specific discharge and location of corresponding gauges are shown in Supplementary Fig. 2.

We also tested the sensitivity of the results to criterion (2) for the selection of record-breaking and surprising events, by varying the threshold T_{mf}/T_{sl} between 1 and 4. The results of the sensitivity analysis are shown in Supplementary Fig. 3 and indicate that, when the definition of megafloods is extended to less surprising events (that is, $T_{mf}/T_{sl} < 3$), the fraction of megaflooods larger than the envelope is unchanged. The only exception is the Boreal region, where fewer events are selected.

Donor catchments

For each catchment in which a megaflood had occurred (target catchment), a pool of similar catchments (donor catchments) was identified in the same region. The similarity between the catchments was quantified in terms of weighted normalized Euclidean distance D in a three-dimensional space with the following dimensions: the logarithm of catchment area A, the logarithm of the mean of the annual maximum specific discharges q_m normalized to a catchment area of 100 km^2 and the coefficient of variation CV of the annual maximum discharges:

$$D = \sqrt{\alpha\left(\frac{\log A_i - \log A_j}{\mathrm{sd}(\log A)}\right)^2 + \beta\left(\frac{\log q_{m,i} - \log q_{m,j}}{\mathrm{sd}(\log q_m)}\right)^2 + \gamma\left(\frac{\mathrm{CV}_i - \mathrm{CV}_j}{\mathrm{sd}(\mathrm{CV})}\right)^2} \tag{6}$$

where i refers to the target catchment, j to a potential donor catchment and sd is the standard deviation of all catchments in the donor group. Greek letters indicate weights. q_m and CV were calculated on flood data prior to the year of occurrence of the target event to obtain a cross-validation experiment that resembles a case of anticipating

megafloods a priori. In estimating q_m and CV we excluded outliers (for both the target and the donor catchments) according to the criterion of equation (2), because megafloods should not influence the comparison, and only smaller, frequently occurring floods were used, which is the only information usually available in the case of a prediction. The pooling group is identified by setting a maximum distance D_{max}. In selecting the number of catchments in the pooling group, there is a tradeoff between a larger group that has a higher chance of containing very large floods, and a smaller group that is hydrologically more homogeneous. For Figs. 1–3 we used $\alpha = \beta = \gamma = 1$ (corresponding to the assumption of the three dimensions having the same importance) and included catchments with $D < D_{max}$ with $D_{max} = 1$, guided by a sensitivity analysis (see below and Extended Data Fig. 2).

Megaflood prediction

We repeated the selection of the donor group for each target catchment and estimated the envelope curve, using the slope b of the corresponding hydroclimatic region and the intercept determined as the minimum that satisfies the envelope condition of the group only. The procedure only uses observations from donor catchments up to the year before the megaflood in the target catchment (Fig. 2a–c). We finally obtained an estimate of the discharge of a potential megaflood in the target catchment (predicted megaflood) from the envelope curve and compared it to the discharge of the observed megaflood (Fig. 4a).

To evaluate the plausibility of the donor selection, we analysed the timing of the megafloods observed in the target and donor catchments using previously established methods[22] (Fig. 4c). We compared the distribution of the timing of the observed megafloods to the average timing of the ten largest floods in the donor group. The circular distributions in Fig. 4c were obtained using the R circular package.

To evaluate the robustness of the method, we conducted a number of sensitivity analyses. We varied D_{max} between 0.5 and 1.5 and showed that an increase in D_{max} translates into an increasing number of target megafloods that are below the envelope (Extended Data Fig. 2). The larger fraction in the Boreal region is because of fewer donors available compared with the other regions. We also tested the sensitivity of α, β and γ, examining four weight combinations: equal weights ($\alpha = \beta = \gamma = 1$) and doubling one of the weights ($\alpha = 2$ and $\beta = \gamma = 1$; $\alpha = \gamma = 1$ and $\beta = 2$; $\alpha = \beta = 1$ and $\gamma = 2$), which corresponds to the hypothesis of one dimension being more important than the others in the donor selection. There is very little effect on the number of target megafloods below the envelope (Extended Data Fig. 3). While a different set of parameters may modify some of the donor catchments, the resulting envelope curve changes very little. Finally, we tested the effect of replacing the regional subdivision of Fig. 1 by an alternative subdivision[17]. The analysis shows that the alternative regions may modify the choice of individual donor catchments but, again, the overall conclusions do not change (Extended Data Figs. 4–7).

Data availability

The flood discharge data from the data holders/sources listed in Extended Data Table 1 that were used in this paper are available at https://github.com/tuwhydro/megafloods.

Code availability

The data analysis was performed in R using the supporting packages circular, lubridate, plotrix, quantreg, raster, RColorBrewer, rgdal, rworldmap and scales. The code used can be downloaded from https://github.com/tuwhydro/megafloods.

References

32. Hall, J. et al. A European Flood Database: facilitating comprehensive flood research beyond administrative boundaries. *Proc. Int. Assoc. Hydrol. Sci.* **370**, 89–95 (2015).
33. Roekaerts, M. *The Biogeographical Regions Map of Europe. Basic Principles of its Creation and Overview of its Development* (EEA, 2002).
34. Koenker, R. W. *Quantile Regression* (Cambridge Univ. Press, 2005).
35. Amponsah, W. et al. in *Climate Change, Hazards and Adaptation Options* (eds Leal Filho, W. et al.) 267–276 (Springer, 2020).
36. Tukey, J. W. *Exploratory Data Analysis* (Addison-Wesley, 1977).
37. Hubert, M. & Vandervieren, E. An adjusted boxplot for skewed distributions. *Comput. Stat. Data Anal.* **52**, 5186–5201 (2008).
38. Brys, G., Hubert, M. & Struyf, A. A robust measure of skewness. *J. Comput. Graph. Stat.* **13**, 996–1017 (2004).

Acknowledgements

We acknowledge all flood data providers listed in Extended Data Table 1. G.B. and M. Bertola were supported by the FWF projects 'SPATE' (I 3174, I 4776) and W1219-N22. B.M. and B.G. were supported by the DFG 'SPATE' project (FOR 2416). A.V., P.C., D.G., M. Borga and E.D. were supported by the European Union NextGenerationEU 'RETURN' Extended Partnership (National Recovery and Resilience Plan—NRRP, Mission 4, Component 2, Investment 1.3—D.D. 1243 2/8/2022, PE0000005). S.K. and J.S. were supported by the Slovak Research and Development Agency (number APVV-20-0374) and the VEGA Grant Agency (number 1/0782/21). J.H. and S.T. were supported by the ROBIN (Reference Observatory of Basins for INternational hydrological climate change detection) initiative, with funding from the Natural Environment Research Council (grant number NE/W004038/1). The authors acknowledge the involvement in the data screening process of M. Haas.

Author contributions

G.B. and M. Bertola initiated the study and wrote the first draft of the paper. M. Bertola, G.B., M. Borga, A.C., P.C., E.D., D.G., A.M., A.V. and E.V. designed the study. M. Bertola collated the updated version of the database with the help of most of the co-authors and conducted the analyses. G.B. and M. Bertola interpreted the results in the context of underlying geophysical mechanisms. B.G., M. Boháč, A.C., S.K., O.L., S.L. M.M.-G., K.G., Z.G., B.G., J.K., B.M., P.M., J.P., L.P., I.R., K.S., J.S., P.V., P. Ward, P. Willems. and N.Ž. interpreted the results in Central Europe. G.T.A., O.B., M. Borga, A.C., I.Č., G.B.C., P.C., E.D., D.G., A.G., A.M., L.M., D.O., M.Š., A.V. and E.V. interpreted the results in Southern Europe. B.A., B.K., D.L. and N.V. interpreted the results in Northern Europe. J.H., S.H., C.M., S.T. and E.S. interpreted the results in Western Europe. I.D., N.F., L.G., M.K., J.K., M.O. and V.O. interpreted the results in Eastern Europe. All authors contributed to framing and revising the paper.

Competing interests

The authors declare no competing interests.

Additional information

Extended data is available for this paper at https://doi.org/10.1038/s41561-023-01300-5.

Supplementary information The online version contains supplementary material available at https://doi.org/10.1038/s41561-023-01300-5.

Correspondence and requests for materials should be addressed to Miriam Bertola.

Peer review information *Nature Geoscience* thanks the anonymous reviewers for their contribution to the peer review of this work. Primary Handling Editor: Tom Richardson, in collaboration with the *Nature Geoscience* team.

https://doi.org/10.1038/s41561-023-01300-5

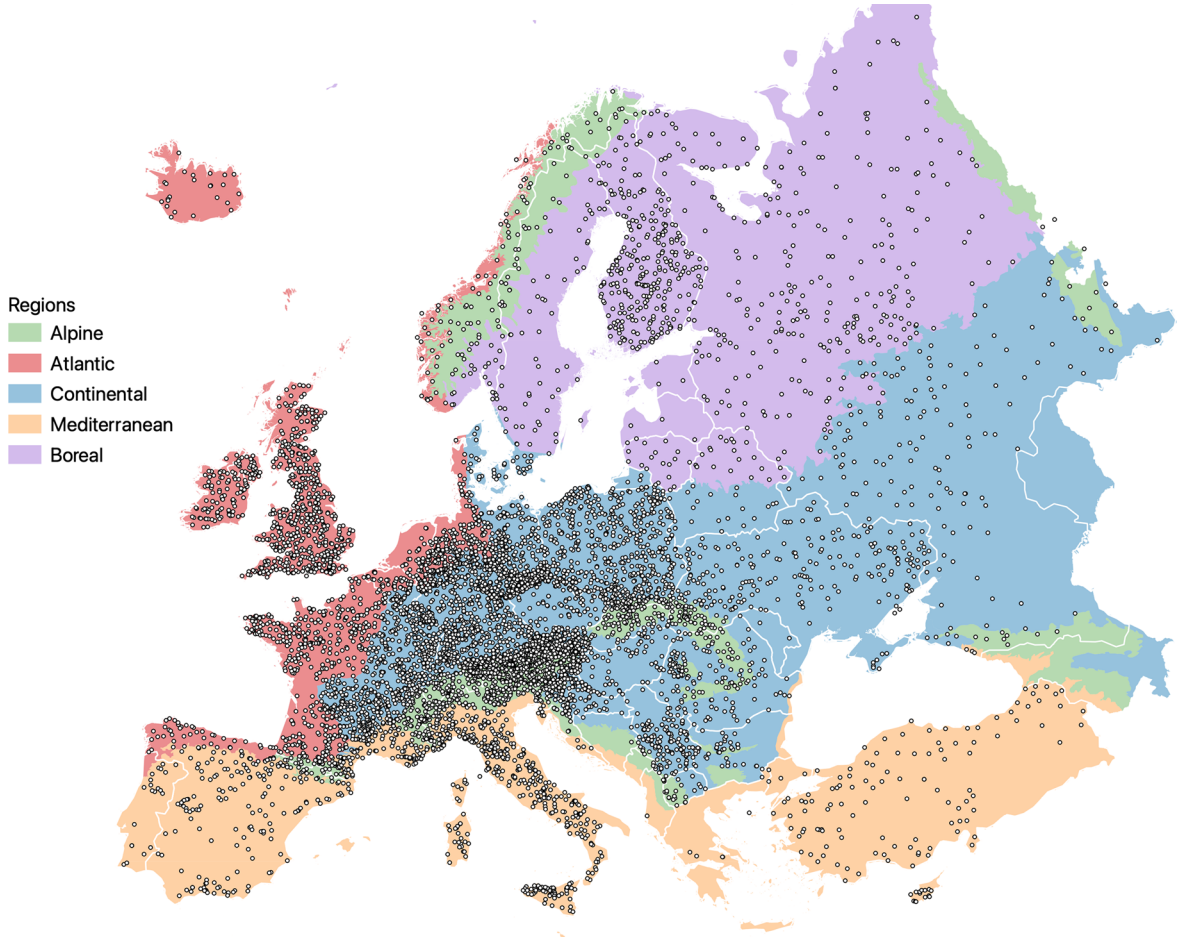

Extended Data Fig. 1 | Map of the European study area. Background colours indicate five European hydroclimatic regions. Open circles indicate the location of the 8,023 hydrometric stations analysed.

https://doi.org/10.1038/s41561-023-01300-5

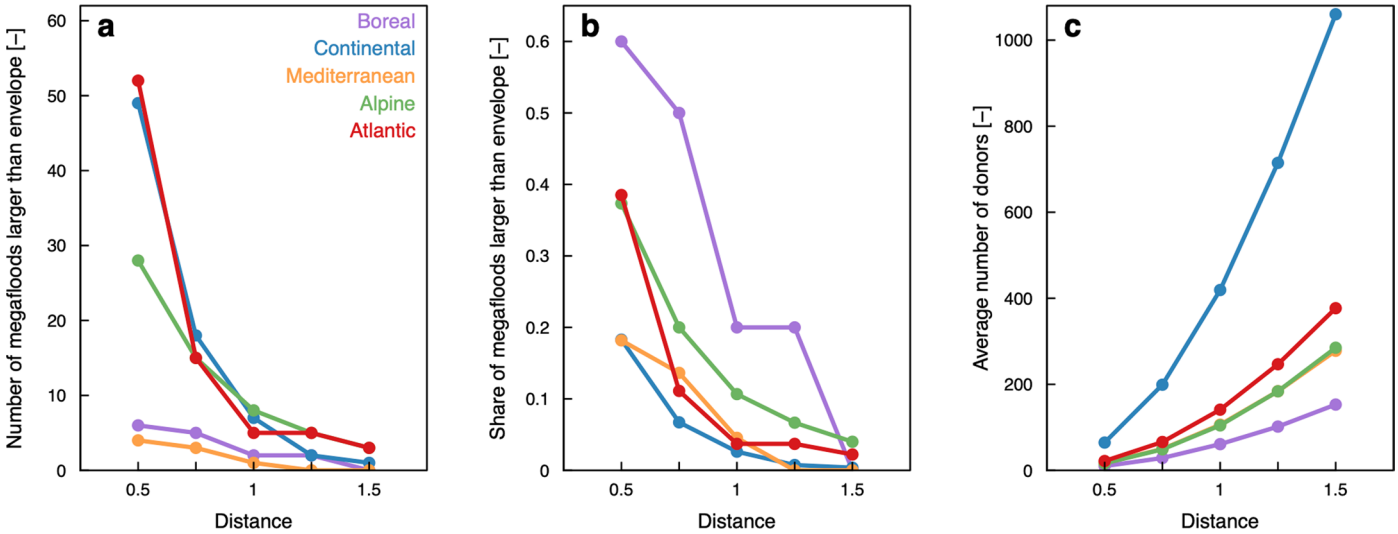

Extended Data Fig. 2 | Sensitivity of results to the threshold distance D_{max}. **(a)** Number and **(b)** fraction of megafloods larger than envelope as a function of threshold distance; **(c)** average number of donor catchments as a function of threshold distance. Colours indicate the five hydroclimatic regions in Europe.

https://doi.org/10.1038/s41561-023-01300-5

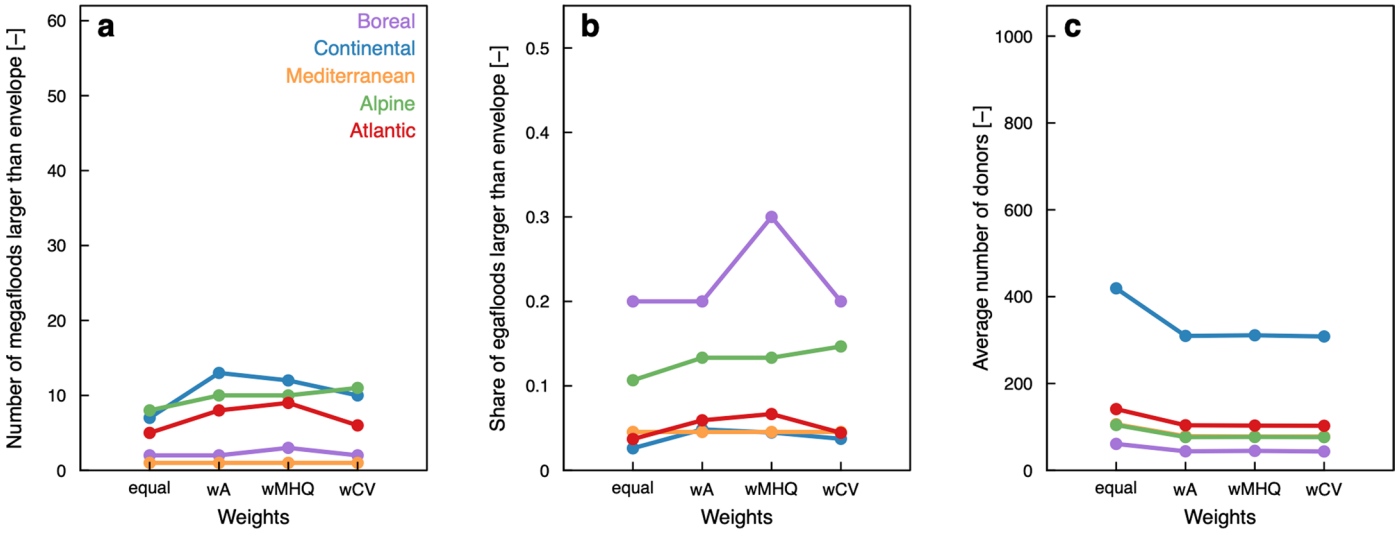

Extended Data Fig. 3 | Sensitivity of results to the weights used for estimating distance D. (a) Number and **(b)** fraction of megafloods larger than envelope for four weight combinations: equal weights ('equal', $\alpha = \beta = \gamma = 1$), double weight for Area ('wA', $\alpha = 2$), double weight for mean annual flood ('wQm', $\beta = 2$), double weight for CV ('wCV', $\gamma = 2$). **(c)** Average number of donor catchments for the four weight combinations. Colours indicate the five hydroclimatic regions in Europe.

https://doi.org/10.1038/s41561-023-01300-5

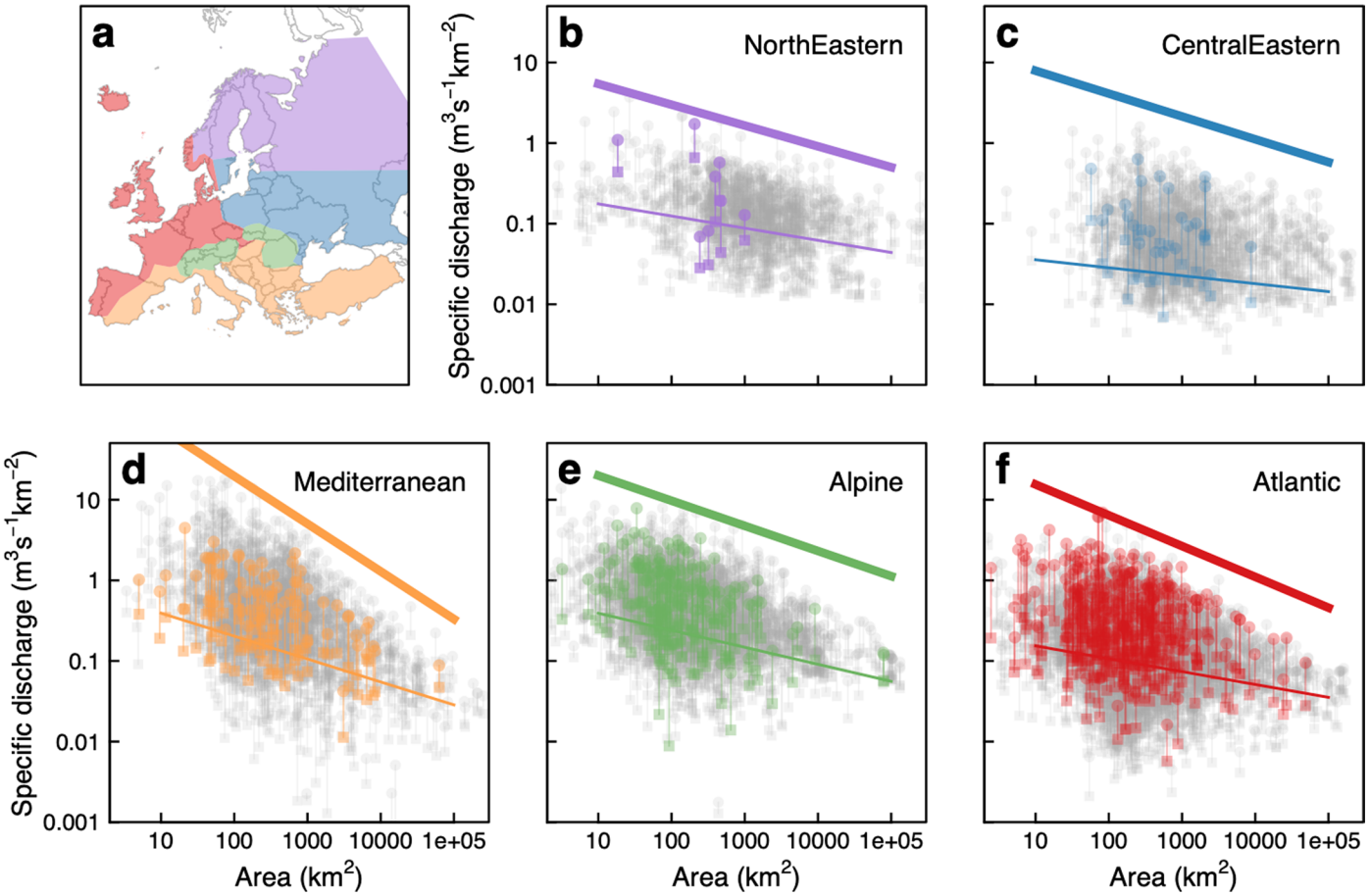

Extended Data Fig. 4 | Megafloods in Europe for alternative hydroclimatic regions. (a) Five alternative hydroclimatic regions[17]. (**b**–**f**) Maximum observed specific flood discharges (points) and mean of annual specific flood discharges (squares) over the entire observation period at each stream gauge as a function of catchment area. Regional envelope curves (thick lines) and median regional annual specific flood discharges (thin lines) are shown for each hydroclimatic region.

https://doi.org/10.1038/s41561-023-01300-5

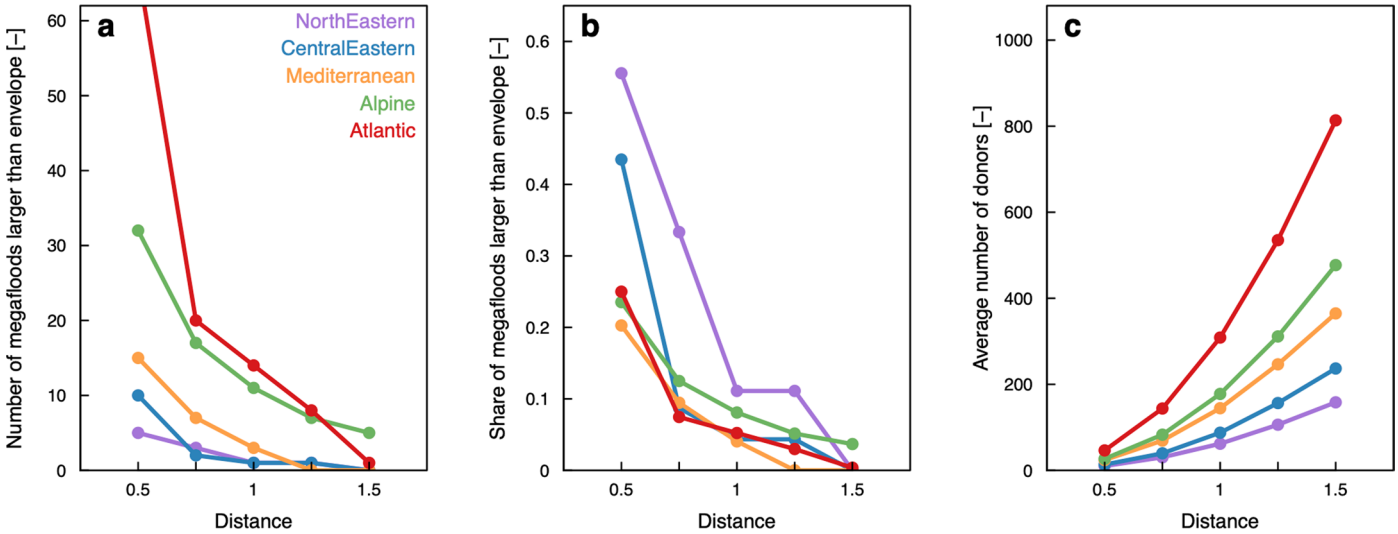

Extended Data Fig. 5 | Sensitivity of results to the threshold distance D_{max}. **(a)** Number and **(b)** fraction of megafloods larger than envelope as a function of threshold distance; **(c)** average number of donor catchments as a function of threshold distance. Colours indicate the five alternative regions of Extended Data Fig. 4a.

https://doi.org/10.1038/s41561-023-01300-5

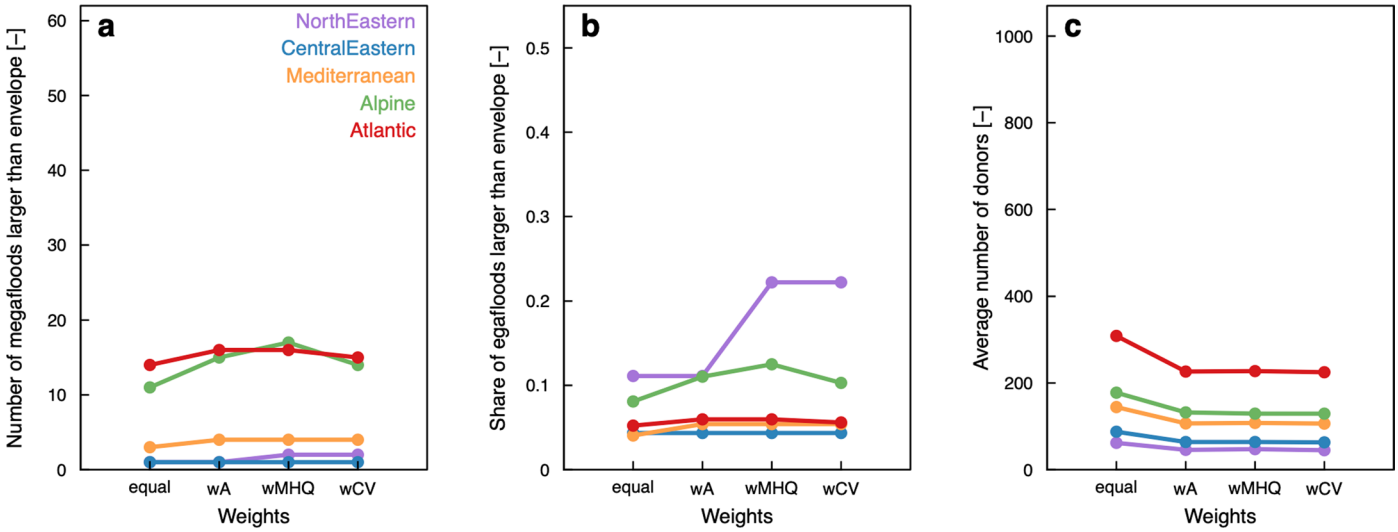

Extended Data Fig. 6 | Sensitivity of results to the weights used for estimating distance D. (a) Number and **(b)** fraction of megafloods larger than envelope for four weight combinations: equal weights ('equal', $\alpha = \beta = \gamma = 1$), double weight for Area ('wA', $\alpha = 2$), double weight for mean annual flood ('wQm', $\beta = 2$), double weight for CV ('wCV', $\gamma = 2$). **(c)** Average number of donor catchments for the four weight combinations. Colours indicate the five alternative regions of Extended Data Fig. 4a.

https://doi.org/10.1038/s41561-023-01300-5

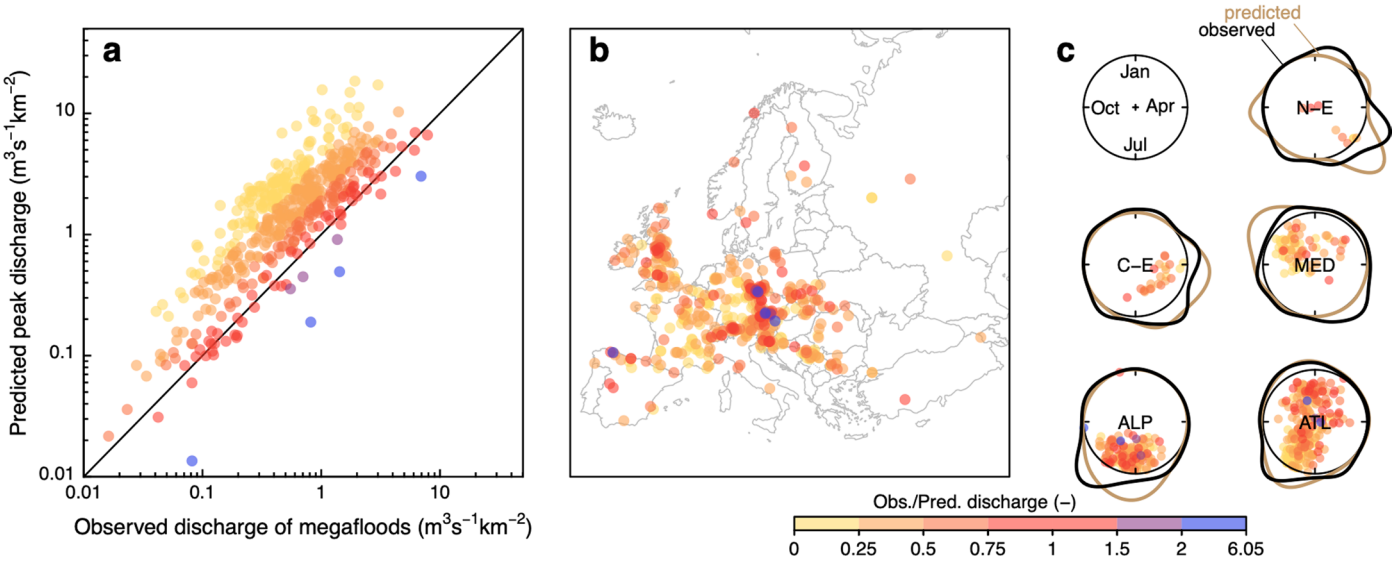

Extended Data Fig. 7 | Predicted versus observed megafloods. Similar to Fig. 4 but for the five alternative regions of Extended Data Fig. 4a. **a**, Predicted specific envelope discharge for 498 target catchments versus observed specific discharge of the megafloods in the same catchments. Predicted envelope discharges are estimated using discharge observations from a pool of donor catchments up to the year before the target megaflood. Colours indicate the ratio of observed and predicted discharge. **b**, Location of target catchments. Megafloods occur all over Europe and are less surprising than commonly assumed. **c**, Circular distribution of the timing of the megafloods observed in the target catchments (black lines), and mean timing of the ten largest floods in the donor catchments (coloured points) and their distribution (brown lines). The distance of the points to the centre is inversely proportional to the standard deviation of the flood timing. N-E, North-Eastern; C-E, Central-Eastern; MED, Mediterranean; ALP, Alpine; ATL, Atlantic.

https://doi.org/10.1038/s41561-023-01300-5

Extended Data Table 1 | Data sources included in the European Flood Database

Country/Project	Data holder/Source/Project information
Albania	National Hydro-Meteorological Service Albania, Institute of GeoSciences, Energy, Water and Environment (IGEWE)
Austria	Hydrographic Services of Austria (HZB)
Belgium	Service Public de Wallonie (SPW)
Belgium	Flemish Environment Agency (VMM)
Belgium	Hydrological Information Service (HIC)
Bosnia and Herzegovina	Hydrological Yearbooks of the former Republic of Yugoslavia
Bulgaria	Hydrological Yearbooks of the Rivers in Bulgaria, National Institute of Meteorology and Hydrology
Croatia	Croatian Meteorological and Hydrological Service
Czechia	Czech Hydrometeorological Institute (CHMI)
Denmark	Danish Centre for Environment and Energy (DCE)
Estonia	Estonian Environment Agency
EWA	European Water Archive (EWA)
Finland	Finnish Environment Institute, Open information/Hydrology/Discharge Source: SYKE
France	Hydroportail database, SCHAPI, French Ministry of Ecological Transition
Germany	Federal Waterways and Shipping Administration (WSV)
Germany, Baden-Wuerttemberg	Ministry for the Environment, Climate and Energy of the Federal State of Baden-Wuerttemberg (LUBW)
Germany, Bavaria	Flood Information Centre, Bavarian Environment Agency, Munich (LfU)
Germany, Brandenburg	Ministry of Rural Development, Environment and Agriculture of the Federal State of Brandenburg (MLUL)
Germany, Hessia	Hessian Agency for Nature Conservation, Environment and Geology (HLNUG)
Germany, Lower Saxony	Lower Saxony Water Management, Coastal Defence and Nature Conservation Agency (NLWKN)
Germany, Mecklenburg-W. Pomerania	State Office of Environment, Nature Protection and Geology of Mecklenburg-Western Pomerania (LUNG)
Germany, North Rhine-Westphalia	State Agency for Nature, Environment and Consumer Protection (LANUV)
Germany, Rhineland-Palatinate	State Office for the Environment, Water Management and Commerce Inspectorate Rhineland-Palatinate (LUWG)
Germany, Saarland	The Saarland State Office for Environmental and Labour Protection (LUA)
Germany, Saxony	Saxon State Agency for Environment, Agriculture and Geology (LfULG)
Germany, Saxony-Anhalt	State Agency for Flood Defence and Water Management of Saxony-Anhalt (LHW)
Germany, Schleswig-Holstein	Schleswig-Holstein Agency for Coastal Defence, National Park and Marine Conservation (LKN.SH)
Germany, Thuringia	Thuringian Regional Office for the Environment and Geology (TLUG)
GRDC	The Global Runoff Data Centre, Koblenz, Germany
Greece	National Data Bank of Hydrological & Meteorological Information (NDBHMI)
Hungary	General Directorate of Water Management, Hungary
HYDRATE	EU-FP7 HYDRATE data: Hydrometeorological data resources and technology for effective flash flood forecasting
Iceland	Icelandic Meteorological Office, Hydrological Database, No. 2013-10-27/01
Ireland	Irish Environmental Protection Agency (EPA)
Ireland	Office of Public Works (OPW)
Italy	CUBIST database, former SIMN (Servizio Idrografico e Mareografico Nazionale)
Italy	National Research Council - Consiglio Nazionale delle Ricerche (CNR)
Italy	ENEL (Ente Nazionale per l'Energia ELettrica)
Italy	AdBPo (Autorità di Bacino del Fiume Po)
Italy	IRPI (Istituto di Ricerca per la Protezione Idrogeologica)
Italy	ISPRA (Istituto Superiore per la Protezione e la Ricerca Ambientale)
Italy, Emilia-Romagna Region	ARPA (Agenzia Regionale per la Protezione dell' Ambiente) Emilia-Romagna
Italy, Piedmont Region	ARPA Piemonte
Italy, Lazio Region	Uffico Idrografico e Mareografico di Roma - Regione Lazio
Italy, Sicily Region	Osservatorio delle Acque della Regione Siciliana
Italy, South Tyrol Region	Hydrographic Office, Autonomous Province of Bolzano
Italy, Trentino Region	Dipartimento Protezione Civile, Provincia Autonoma di Trento
Italy, Umbria Region	Ufficio Idrografico - Regione Umbria
Italy, Veneto Region	ARPA Veneto
Latvia	Latvian Environment, Geology and Meteorology Centre, State Ltd.
Lithuania	Lithuanian Hydrometeorological Service
Macedonia	Macedonian Hydrometeorological Service
Netherlands	Rijkswaterstaat - Dutch Ministry of Infrastructure and the Environment
Norway	Norwegian Water Resources and Energy Directorate - Norges vassdrags- og energidirektorat (NVE)
Poland	Institute of Meteorology and Water Management National Research Institute (IMGW-PIB)
Portugal	Portuguese Environmental Agency, National Information System for Water Resources of Portugal (SNIRH)
Romania	National Institute of Hydrology and Water Management - NIHWM
Russia	The main hydrological characteristics, 1963-1970, 1971-75, 1975-1980, 1980-2000 Ministry of Natural Resources and Ecology of the Russian Federation, State Hydrological Institute
Russia	State Water Cadastre, 1985-2010, State Hydrological Institute, Lomonosov Moscow State University
Russia	Automated information system of state water bodies monitoring (AIS GMVO), Federal Agency for Water Resources
Serbia	Republic Hydrometeorological Service of Serbia (RHSS), Hydrological Yearbooks of Surface Water, Belgrade
Slovakia	Slovak Hydrometeorological Institute (SHMI)
Slovenia	Slovenian Environment Agency (ARSO)
Spain	Centre for Hydrographic Studies (Centro de Estudios Hidrográficos) of CEDEX, Spain
Spain	Automatic Systems of Hydrological Information (SAIH) of the Cantábrico, Ebro, Guadalquivir, Júcar, Miño-Sil, Segura and Tajo River Basins, and of the Andalusian (HidroSur), Catalonia and Galician regions
Sweden	Swedish Meteorological and Hydrological Institute (SMHI)
Switzerland	Federal Office for the Environment (FOEN) / (BAFU)
Turkey	General Directorate of State Hydraulic Works (DSI), Turkey
Ukraine	Hydrological Department, Ukrainian Hydrometeorological Institute (UHMI)
Ukraine	Hydrometeorological Institute, Odessa State Environmental University (OSENU)
United Kingdom	UK National River Flow Archive (NRFA)

https://doi.org/10.1038/s41561-023-01300-5

Extended Data Table 2 | Parameters of envelope curves and median regression

Region	Slope envelope *b*	Intercept envelope *a*	Envelope specific discharge at 1000 km^2 (m^{3}s^{-1}km^{-2})	Slope median regression *b*	Intercept median regression *a*
Boreal	-0.07 (-0.06/-0.05)	0.36 (0.32/-0.03)	1.37 (1.35/0.66)	-0.09 (-0.11/-0.09)	-0.88 (-0.80/-0.94)
Continental	-0.38 (-0.39/-0.40)	1.49 (1.50/1.45)	2.17 (2.13/1.79)	-0.22 (-0.23/-0.24)	-0.55 (-0.52/-0.52)
Mediterranean	-0.57 (-0.58/-0.41)	2.42 (2.25/2.06)	5.26 (3.16/6.91)	-0.28 (-0.29/-0.29)	-0.02 (-0.05/-0.11)
Alpine	-0.27 (-0.22/-0.33)	1.49 (1.35/1.52)	4.76 (4.94/3.35)	-0.20 (-0.20/-0.21)	-0.18 (-0.20/-0.15)
Atlantic	-0.34 (-0.30/-0.34)	1.49 (1.31/1.50)	2.98 (2.50/2.93)	-0.15 (-0.14/-0.14)	-0.65 (-0.68/-0.67)

The units used in Eq. 1 for estimating the envelopes are q (m^{3}s^{-1}km^{-2}) and A (km^2). Numbers in brackets refer to the first and second sub-periods.

https://doi.org/10.1038/s41561-023-01300-5

Extended Data Table 3 | Relationship of megafloods and mean annual floods in the same catchment

	All catchments		Target catchments (i.e. those with megafloods)	
Region	**Number of stream gauges**	**Average ratio maximum discharge / mean discharge**	**Number of stream gauges**	**Average ratio megaflood / mean discharge**
Boreal	671	2.09	9 (1.3%)	2.78
Continental	3660	3.25	263 (7.2%)	5.28
Mediterranean	938	3.50	21 (2.2%)	5.20
Alpine	1240	2.83	74 (6.0%)	3.94
Atlantic	1514	2.36	131 (8.7%)	3.38

The table refers to the points and squares in Fig. 1.